

Loss of dentin sialophosphoprotein leads to periodontal diseases in mice

M. P. Gibson¹, Q. Zhu^{1,2},
Q. Liu¹, R. N. D'Souza¹,
J. Q. Feng¹, C. Qin¹

¹Department of Biomedical Sciences, Baylor College of Dentistry, Texas A&M Health Science Center, Dallas, TX, USA and ²Department of Operative Dentistry and Endodontics, the Fourth Military Medical University, School of Stomatology, Xi'an, Shaanxi, China

Gibson MP, Zhu Q, Liu Q, D'Souza RN, Feng JQ, Qin C. Loss of dentin sialophosphoprotein (DSPP) leads to periodontal diseases in mice. *J Periodont Res* 2013; 48: 221–227. © 2012 John Wiley & Sons A/S

Background and Objective: Dentin sialophosphoprotein (DSPP) and its cleaved products, dentin phosphoprotein (DPP) and dentin sialoprotein (DSP), play important roles in biomineralization. Recently, we observed that DSPP is highly expressed in the alveolar bone and cementum, indicating that this molecule may play an important role in the formation and maintenance of a healthy periodontium, and its deletion may cause increased susceptibility to periodontal diseases. The objective of this investigation was to study the effects of *Dspp* ablation on periodontal tissues by analyzing *Dspp* null mice.

Material and Methods: Newborn to 6-mo-old *Dspp* null mice were examined, and the 3- and 6-mo-old *Dspp* null mice were characterized in detail using X-ray radiography, histology and scanning electron microscopy (backscattered as well as resin-infiltrating). Wild-type mice of the same age groups served as the normal controls.

Results: The *Dspp* null mice showed significant loss of alveolar bone and cementum, particularly in the furcation and interproximal regions of the molars. The alveolar bone appeared porous while the quantity of cementum was reduced in the apical region. The canalicular systems and osteocytes in the alveolar bone were abnormal, with reduced numbers of canaliculi and altered osteocyte morphology. The loss of alveolar bone and cementum along with the detachment of the periodontal ligaments (PDL) led to the apical migration of the epithelial attachment and formation of periodontal pockets.

Conclusion: Inactivation of DSPP leads to the loss of alveolar bone and cementum and increased susceptibility to bacterial infections in PDL of *Dspp* null mice. The fact that the loss of DSPP results in periodontal diseases indicates that this molecule plays a vital role in maintaining the health of the periodontium.

Chunlin Qin, DDS, PhD, Department of Biomedical Sciences, Baylor College of Dentistry, 3302 Gaston Avenue, Room 452, Dallas, TX 75246, USA
Tel: +214 828 8292
Fax: +214 874 4538
e-mail: cqin@bcd.tamhsc.edu

Key words: alveolar bone; cementoblast; dentin; osteocyte; periodontal attachment; periodontal disease

Accepted for publication July 12, 2012

Dentin phosphoprotein (DPP) with a very high level of phosphorylation was discovered in 1967 (1), while dentin sialoprotein (DSP), a glycoprotein with little or no phosphate, was identified in 1981(2). Both proteins were believed to be separate entities until the discovery of a single gene (*Dspp*) that encodes both DSP and DPP (3).

Dentin sialophosphoprotein (DSPP) belongs to a family of non-collagenous proteins known as SIBLING (Small Integrin-Binding Ligand, N-linked Glycoprotein) (4). The SIBLING family members share a number of similarities in their genomic organization, post-translational modifications and tissue localization. Other

members of this family include osteopontin, bone sialoprotein, dentin matrix protein 1 (DMP1), and matrix extracellular phosphoglycoprotein (5).

The importance of DSPP in biomineralization has been illustrated in human and mouse genetic studies that revealed the association of *Dspp* mutations or ablations with mineralization

defects in the dentin and bone (6–9). Originally thought to be dentin-specific, DSPP was later found in bone, cementum and a number of non-mineralized tissues (10–18). Previous studies in our group showed that the expression of DSPP in the alveolar bone and cementum is remarkably higher than in the long bone (12,18). The high expression level of DSPP in these two periodontal tissues led us to believe that this molecule may play important roles in the formation and maintenance of a healthy periodontium, and its deletion may cause increased susceptibility to periodontal diseases. The aim of this investigation was to study the effects of DSPP on periodontal tissues by comparing periodontal tissues of *Dspp* null mice with those of wild-type (WT) mice at different ages.

Materials and methods

Animals and tissue acquisition

In this study, we thoroughly characterized 3- and 6-mo-old *Dspp* knockout (*Dspp* null) mice (strain name: B6; 129-Dspp^{tm1Kul}/Mmnc; MMRRC, UNC, Chapel Hill, NC, USA). For control purposes, we used the same age WT male C57BL/6J mice (The Jackson Laboratory, Bar Harbor, ME, USA). The animal protocol used in this study was approved by the Animal Welfare Committee of Texas A&M Health Science Center Baylor College of Dentistry (Dallas, TX, USA).

Plain X-ray radiography and micro-computed tomography

The mandibles were dissected from the WT as well as the *Dspp* null mice at 3 mo and 6 mo. The dissected samples were analyzed by plain X-ray radiography (MX-40; Faxitron, Lincolnshire, IL, USA) and micro-computed tomography (μ -CT) using a μ -CT35 imaging system (Scanco Medical, Bassersdorf, Switzerland). The μ -CT analyses included (i) a medium-resolution scan (7.0 μ m slice increment) of the whole mandible from the 3- and 6-mo-old mice for an overall assessment of the shape and structure, and (ii) a high-

resolution scan (3.5 μ m slice increment) of the alveolar bone region. For the quantitative analysis of alveolar bone and to determine the bone volume fraction, we selected a cylindrical region starting at the furcation area and between the medial and distal root of the first mandibular molar with a fixed radius and length for all samples. The data acquired from the high-resolution scans for five samples per group ($n = 5$) were then used for quantitative analyses using the Student's *t*-test. $p < 0.05$ was considered statistically significant, and the data are presented as mean \pm SD.

Histology

Under anesthesia, 3- and 6-mo-old WT and *Dspp* null mice were perfused from the ascending aorta with 4% paraformaldehyde in 0.1 M phosphate buffer. The mandibles were dissected and further fixed in the same fixative for 48 h, followed by demineralization in 8% EDTA containing 0.18 M sucrose (pH 7.4) at 4°C for 2 wks. The tissues were processed for paraffin embedding, and serial 5- μ m sections were prepared. Sections were stained with hematoxylin and eosin.

Backscattered, and resin infiltration and acid etching scanning electron microscopy

The mandibles from the 3-mo-old WT and *Dspp* null mice were dissected, fixed in 2% paraformaldehyde and 2.5% glutaraldehyde in 0.1 M cacodylate buffer solution (pH 7.4) at room temperature for 4 h and then transferred to 0.1 M cacodylate buffer solution. The tissue specimens were dehydrated in ascending concentrations of ethanol and then embedded in methyl methacrylate (Buehler, Lake Bluff, IL, USA). Sandpaper was used to grind the acrylic block in increasing order of grit fineness. Samples were then polished with a micro cloth with Metadi Supreme Polycrystalline diamond suspensions of decreasing sizes (0.1 μ m, 0.25 μ m and 0.05 μ m). These samples were then washed in the ultrasonic wash and placed in the vacuum system overnight.

For backscattered scanning electron microscopy (SEM), the surfaces of the methyl methacrylate-embedded mandibles were polished and then coated with carbon. The specimens were examined with a FEI/Philips XL30 Field emission environmental SEM (Philips, Hillsboro, OR, USA). Subsequently, the surface was acid etched with 37% phosphoric acid for 2–10 s, followed by 5.25% sodium hypochlorite treatment for 5 min. The specimens were then coated with gold and palladium, and examined with SEM.

Results

Plain X-ray radiography and micro-computed tomography

Plain X-ray radiography revealed alveolar bone loss in the mandibular molar furcation as well as in the interdental region of the *Dspp* null mice at 3 mo of age (Fig. 1A and 1B). The destruction of alveolar bone in these mice was even more evident in the 6-mo-old mice compared to the WT mice (Fig. 1C and 1D). Widening of the periodontal space in the apical region of the molars was also observed in both age groups of the *Dspp* null mice (Fig. 1B and 1D).

The μ -CT analyses further demonstrated the loss of alveolar bone in the *Dspp* null mice (Fig. 2). At 3 mo, the alveolar bone in these mice appeared more porous interdentally in the mandibular molar region (Fig. 2A and 2B). The longitudinal section view of the same region also revealed alveolar bone defects and porosities in the *Dspp* null mice compared with the WT mice (Fig. 2C and 2D). The alveolar bone defects became more striking as the mice aged, and the 6-mo-old *Dspp* null mice showed more severe alveolar bone defects and porosities (Fig. 2E to 2H) than did the 3-mo-old mice. The longitudinal section revealed more severe alveolar bone loss in the 6-mo-old *Dspp* null mice (Fig. 2G and 2H). Quantitative analysis showed a significant ($p < 0.05$) decrease in the ratio of alveolar bone volume to total volume in the *Dspp* null mice (Fig. 2I).

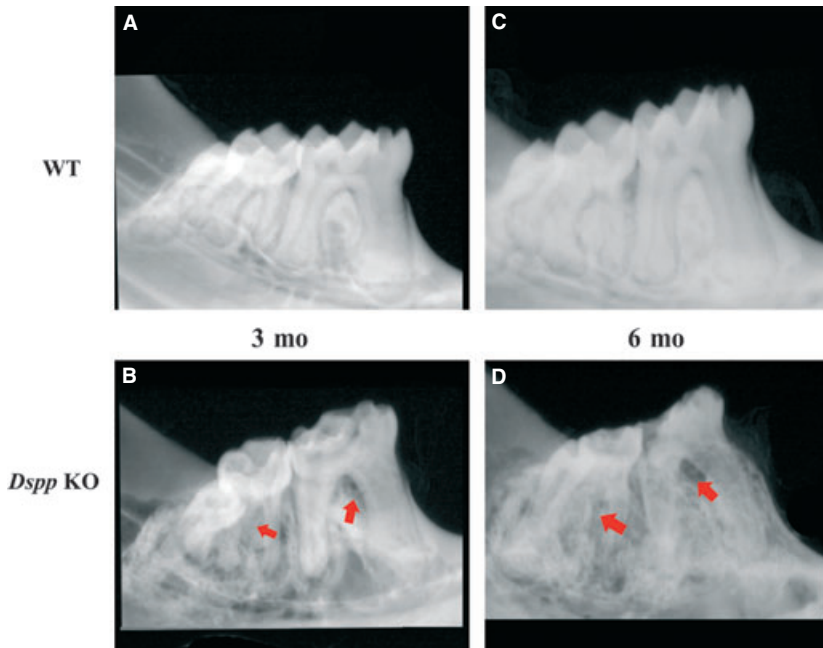


Fig. 1. Plain X-ray radiography. Mandibles from 3- and 6-mo-old WT and *Dspp* null mice were analyzed by plain X-ray radiography. Comparison between the mandibles of 3-mo-old WT (A) and *Dspp* null (B) showed alveolar bone loss in the furcation and interdental region (red arrows) of the first and second molars in the *Dspp* null mice (B). These regions in the *Dspp* null mice were more radiolucent compared to the same age WT controls. Apically, the mandibular molars of the *Dspp* null mice (B) also showed widened radiolucent areas indicating widening of the periodontal space. Comparison between the WT and *Dspp* null mandibles (C and D) at 6 mo of age revealed even more profound alveolar bone loss in the mandibular molar furcation as well as in the interdental region (red arrowhead) of the *Dspp* null mice. KO, knockout; WT, wild type.

Histological evaluation

Hematoxylin and eosin staining demonstrated severe alveolar bone loss along with infiltration of inflammatory cells and detachment of junctional epithelium in both the 3- and 6-mo-old *Dspp* null mice (Fig. 3), indicating the development of periodontal diseases.

At 3 mo, the *Dspp* null mice showed alveolar bone loss in the furcation region of the first mandibular molar (Fig. 3A and 3B) compared to the WT mice. There was also an increase in the number of inflammatory cells in the same region (Fig. 3A and 3B). The histology analyses showed a remarkable loss of alveolar bone and disruption of periodontal ligaments in the *Dspp* null mice, along with the apical migration of the junctional epithelium almost to the level of the alveolar bone crest in the interdental region between the first and second mandibular molars (Fig. 3C

and 3D). In 6-mo-old *Dspp* null mice, bone loss in the furcation (Fig. 3E and 3F) and interdental regions (Fig. 3G and 3H) of the mandibular first molar was worse than in the 3-mo-old mice; severe inflammatory cell infiltration was observed in these regions as well as more significant apical migration of the epithelial attachment and severe interdental alveolar bone loss. In the *Dspp* null mice, the alveolar bone loss appeared in both vertical and horizontal directions. No pulp exposure was observed in these animals and, therefore, the periodontal defects and presence of inflammatory cells were not associated with pulpitis.

Backscattered scanning electron microscopy, and resin infiltration and acid scanning electron microscopy

Using backscattered SEM, we observed an overall loss of alveolar

bone and cementum in the mandibular first molar and incisor region of the 3-mo-old *Dspp* null mice (Fig. 4B) compared with the WT mice of the same age (Fig. 4A). The periapical region of the mandibular first molar in the *Dspp* null mice showed a significant loss of cementum (Fig. 4D) compared with the WT mice, which have an abundant thickness of cementum in the region (Fig. 4C). In the same region, WT mice showed an even distribution of the mineral surrounding the osteocyte lacunae in the alveolar bone (Fig. 4E and 4F), while the mineral was significantly reduced in a similar region surrounding the osteocytes in the *Dspp* null mice (Fig. 4G and 4H).

To further evaluate the morphological changes of the osteocytes and lacuna–canalicular system of the alveolar bone as well as the morphology of the cementum in *Dspp* null mice, the resin-infiltrated sections were etched by acid to reveal three-dimensional images of the osteocytes (Fig. 5). While the WT sample revealed evenly distributed cementum (Fig. 5A), the *Dspp* null mice displayed little or no cementum (Fig. 5B). The lacunae of the WT osteocytes were highly organized and regularly spaced (Fig. 5C) with a large number of canaliculi running perpendicular to the long axis of the osteocytes (Fig. 5E). In contrast, lacunae of the *Dspp* null osteocytes appeared larger and irregularly distributed with disorganized canaliculi that were fewer in number (Fig. 5D and 5F). These canaliculi had a markedly reduced extension into the surrounding bone (Fig. 5F).

Discussion

Once believed to be a tooth-specific protein, DSPP is now recognized as a constituent of bone, cementum, and a number of non-mineralized tissues (10,11,13–17,19). Previous work in our laboratory showed that the expression level of DSPP in the alveolar bone and cellular cementum is remarkably higher than in the long bone (12,18). In these two tissues, DSPP is found in the osteocytes,

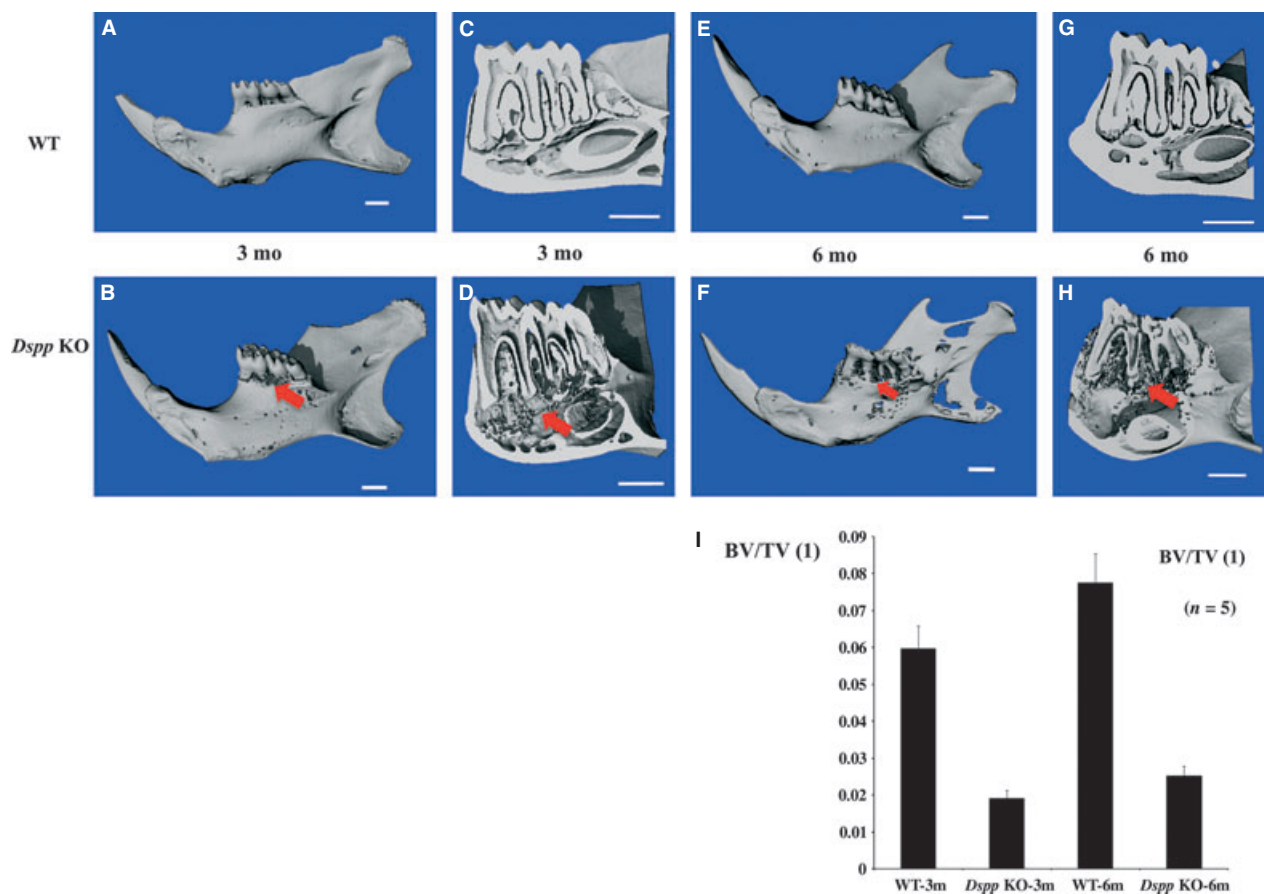


Fig. 2. Micro-computed tomography (μ -CT). The mandibles of 3- and 6-mo-old WT and *Dspp* null mice were analyzed by μ -CT. At 3 mo (A–D), μ -CT images showed the loss of alveolar bone in the *Dspp* null mice (B,D). The alveolar bone in the *Dspp* null mice appeared rough and porous (red arrow) around the mandibular molars (B). A longitudinal section of the mandibular molar region revealed alveolar bone defects and porosities in the *Dspp* null mice (D; red arrow) compared with the WT mice (C). At 6 mo (E–H), the alveolar bone abnormalities became more striking. Note the extensive loss and porosities (pointed by the red arrows) of the alveolar bone (F, H) in the *Dspp* null mice (H). Bar: 1 mm. The quantitative analysis of 3- and 6-mo-old *Dspp* null mice vs. WT mice showed a significant decrease in the ratio of alveolar bone volume to total bone volume (BV/TV) for both age groups (I). $p < 0.05$; data represent mean \pm SD and $n = 5$. KO, knockout; WT, wild type.

cementocytes and the matrices of these cells (12). Studies have indicated that the loss of DSPP leads to an enlarged pulp chamber and to thinner and poorly mineralized dentin (6), while its effects on the health of periodontium have not been studied. In this study, we found that the loss of DSPP activity caused loss of alveolar bone, which was evident from plain X-ray and μ -CT analyses. Histological analyses revealed inflammatory infiltration around the alveolar bone with the loss of interdental bone as well as apical migration of junctional epithelium. SEM data further confirmed the loss of alveolar bone, cementum and reduced propagation of the osteocyte processes into

surrounding bone. It is worth noting that no pulpal exposure was observed in the first molars of these animals and, therefore, periodontal defects and presence of inflammatory cells were not associated with inflammation of the dental pulp. The abnormal morphology of osteocytes in the alveolar bone of *Dspp* knockout mice (Fig. 5) further supports our conclusion that the alveolar bone defects must be due to intrinsic factors of bone cells associated with *Dspp* inactivation and is not caused by inflammation of the dental pulp. Additionally, the bacterial infiltration in PDL worsened at 6 mo of age in these mice following deterioration of periodontal tissues. Our findings in this investiga-

tion demonstrate that inactivation of *Dspp* leads to severe periodontal disease in mice, indicating that DSPP plays a critical role in maintaining the structural integrity of periodontal structures.

Previous studies have reported that mice younger than 12 mo do not naturally develop periodontal diseases and that the diseases in older mice have a higher predilection of occurrence in the maxilla (20). Under normal physiological conditions, these mice ultimately develop periodontal bone loss in the maxilla because of aging (21). In contrast, we showed that the *Dspp* null mice have severe alveolar bone and cementum defects as young as 3 mo, pointing to a very

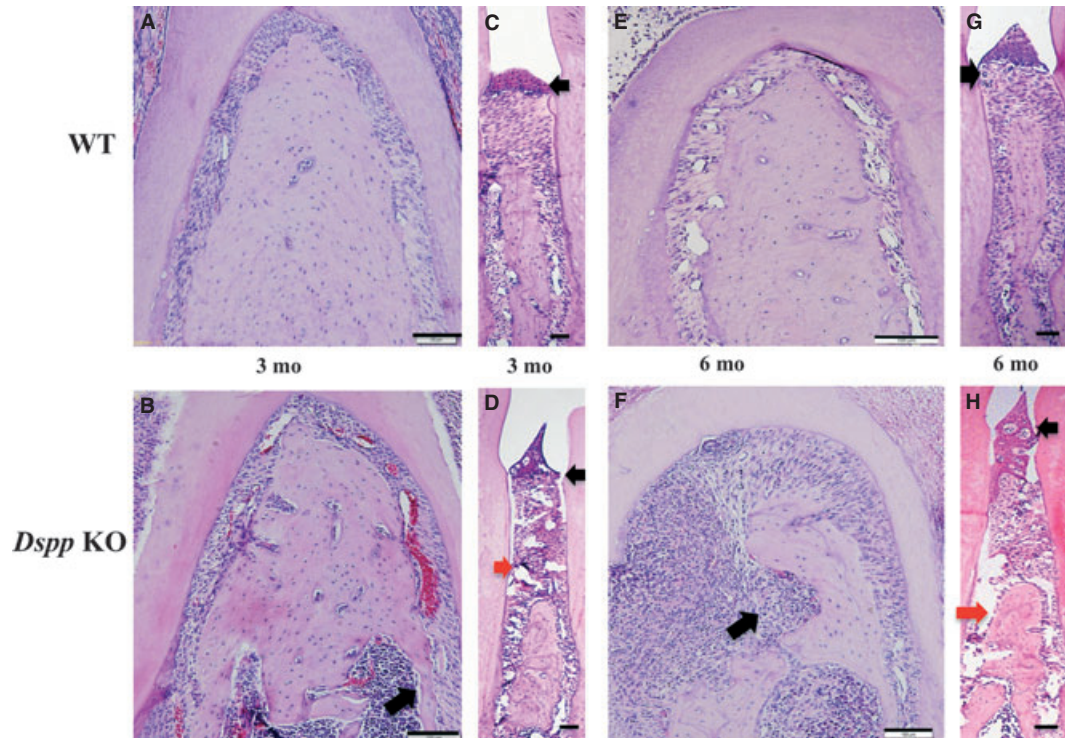


Fig. 3. Hematoxylin and eosin staining. These specimens were from the 3- and 6-mo-old WT and *Dspp* null mandibular molars. At 3 mo, the *Dspp* null mice (B) showed alveolar bone loss in the furcation region of the mandibular first molar with an increase of inflammatory cells (black arrow) compared to the WT mice (A). Interdentally, the epithelial attachment of the WT mice was at the cemento-enamel junction (CEJ) (C, indicated with a black arrow), whereas the *Dspp* null mice had poor alveolar bone in the interdental region with an apically recessed epithelial attachment (D). The black arrows in (C) and (D) indicate the CEJ, and the red arrows mark the actual epithelial attachment recessed significantly from the CEJ (D). At 6 mo, the *Dspp* null mice had more significant alveolar bone loss in the furcation region of the mandibular first molar (F). The inflammatory cells seem to have completely engulfed the bone in the furcation region (F, black arrow). Interdentally the apical recession of the epithelium and bone loss appeared to have progressively worsened with aging in the *Dspp* null mice (H, red arrow). The black arrows represent the CEJ in (G) and (H). Bar: 100 μ m. KO, knockout; WT, wild type.

early breakdown of the periodontal tissues in the mandibular molars of these mutant mice.

Our study shows that periodontal manifestations in *Dspp* null mice are due to defects in the alveolar bone and cementum, which lead to secondary effects on the PDL and eventual bacterial infiltration leading to periodontal diseases with the formation of periodontal pockets. It is interesting that the osteocytes in the *Dspp* null mice display an abnormal shape, along with a reduced number of canaliculi in the surrounding bone. It is hard to know if these phenotypic changes in the periodontal tissues of *Dspp* null mice are due to the postnatal loss of function or due to defects in these cells during embryonic development of the periodontal tissues. However, *Dspp* null and WT mice showed similar amounts of alveolar

bone and cementum at 1 mo of age (data not shown), suggesting that the loss of periodontal tissues may be attributed to the postnatal function loss of the cells responsible for forming alveolar bone and cementum. More studies are warranted to further elucidate this aspect.

Recent studies have shown that the loss of DMP1, another SIBLING member that shares many similarities with DSPP, causes periodontal diseases in mice (22). The periodontal defects in *Dspp* null mice were similar to those of *Dmp1* null mice. However, unlike *Dspp* null, *Dmp1* null mice did not show any clear evidence of inflammation in the alveolar bone of mandibular molars. The *Dspp* null mice in our study exhibited a severe inflammatory reaction in the alveolar bone of the interdental region between the first and second mandib-

ular molars and the furcation region. It has already been shown that DMP1 plays an essential role in the conversion of osteoblasts into mature osteocytes (23–29). The abnormal morphology of the osteocyte lacunae in the *Dspp* null mice suggests that DSPP may also play a vital role in the formation of the lacuna–canalicular system, which is critical to maintaining the health of the alveolar bone. Therefore, similar to DMP1, DSPP may also be needed for the formation and/or function of mature osteocytes in the alveolar bone. The COOH-terminal fragment of DSPP, known as dentin phosphoprotein (DPP) or phosphophoryn has been shown to regulate the expression of the marker genes of bone and dentin via the integrin/MAPK signaling pathway (30) and the Smad pathway (31). Our findings that inactivation of *Dspp* leads

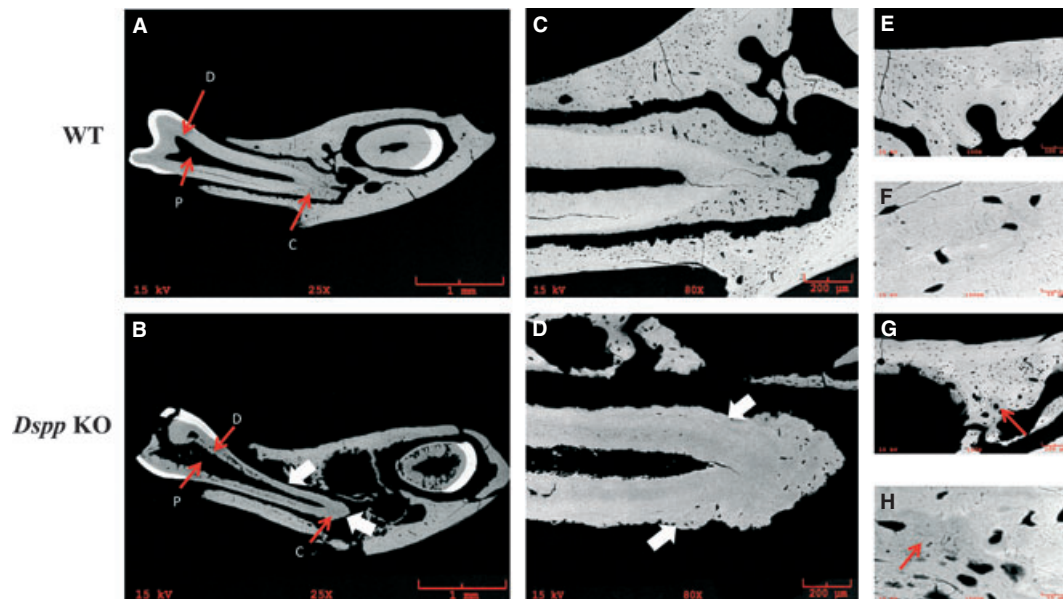


Fig. 4. Backscattered scanning electron microscopy (SEM). Backscattered SEM showed that the mandibular first molar and incisor of the 3-mo-old WT mice (A) had an even distribution of dentin (D), cementum (C) and normal pulp chamber (P). In contrast, the same age *Dspp* null mice (B) had irregular dentin (D), cementum (white arrows, marked as C) and an enlarged pulp chamber (P) as well as loss of alveolar bone. Pulpal exposure of the *Dspp* null mice can be seen in this view, which we believe could be due to loss of the sample while sectioning the methacrylate blocks. The enlarged view of the mandibular first molar periapical region in the WT (C) and *Dspp* null (D) mice revealed a severe loss of cementum (white arrowheads) in the latter. In the WT mice, mineral was evenly distributed around the osteocyte lacunae in the periapical region of the molar (E, F), while the same region of the *Dspp* null mice was poorly mineralized, appearing as a grayish zone (red arrows) surrounding the *Dspp* null osteocytes (G and H). Bar: A, B = 1 mm; C, D = 200 μ m; E, G = 100 μ m; F, H = 10 μ m. KO, knockout; WT, wild type.

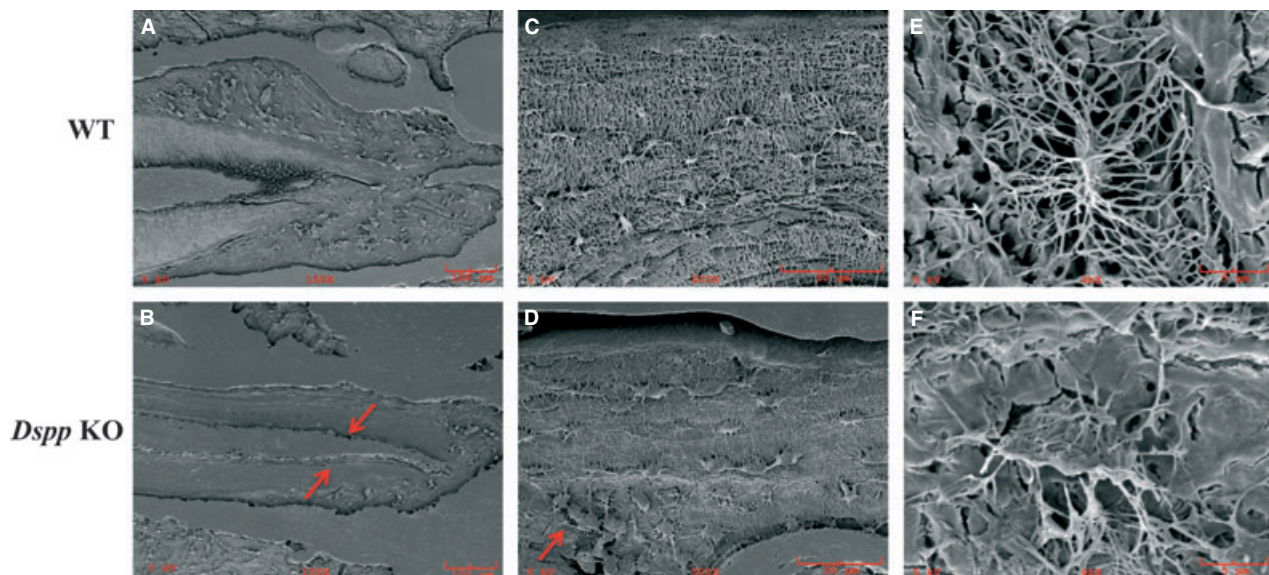


Fig. 5. Resin infiltration and acid etching (SEM). At 3 mo, the WT mice showed evenly distributed cementum (A), whereas there was little or no cementum deposition (B, red arrows) for the *Dspp* null mice. The SEM images showed that the lacunae of the WT osteocytes were highly organized and regularly spaced (C), with numerous canaliculi running perpendicular to the long axis of the osteocyte (E). In contrast, the *Dspp* null osteocyte lacunae appeared larger and irregularly distributed, along with fewer disorganized canaliculi (D, red arrow) in the matrix; these canaliculi appeared to have a markedly reduced propagation into surrounding bone (F). Bar: A, B = 100 μ m; C, D = 50 μ m; E, F = 5 μ m. KO, knockout; WT, wild type.

to intrinsic defects in the alveolar bone are consistent with the conclusion that DSPP and/or DPP is involved in the integrin/MAPK signaling pathway and the Smad pathway, both of which are essential to osteogenesis. Further studies are warranted to uncover the exact mechanisms by which DSPP and/or DPP help to maintain the integrity of the periodontal tissues, including the alveolar bone.

Acknowledgements

This work was supported by Grant DE005092 (to CQ) from the National Institutes of Health. The authors are grateful to Ms. Jeanne Santa Cruz for her assistance with the editing of this article.

References

1. Veis A, Perry A. The phosphoprotein of the dentin matrix. *Biochemistry* 1967; **6**:2409–2416.
2. Butler WT, Bhowm M, Dimuzio MT, Linde A. Noncollagenous proteins of dentin. Isolation and partial characterization of rat dentin proteins and proteoglycans using a three-step preparative method. *Coll Relat Res* 1981; **1**:187–199.
3. MacDougall M, Simmons D, Luan X, Nydegger J, Feng J, Gu TT. Dentin phosphoprotein and dentin sialoprotein are cleavage products expressed from a single transcript coded by a gene on human chromosome 4. Dentin phosphoprotein DNA sequence determination. *J Biol Chem* 1997; **272**:835–842.
4. Fisher LW, Torchia DA, Fohr B, Young MF, Fedarko NS. Flexible structures of SIBLING proteins, bone sialoprotein, and osteopontin. *Biochem Biophys Res Commun* 2001; **280**:460–465.
5. Fisher LW, Fedarko NS. Six genes expressed in bones and teeth encode the current members of the SIBLING family of proteins. *Connect Tissue Res* 2003; **44** (Suppl 1):33–40.
6. Sreenath T, Thyagarajan T, Hall B *et al*. Dentin sialophosphoprotein knockout mouse teeth display widened predentin zone and develop defective dentin mineralization similar to human dentinogenesis imperfecta type III. *J Biol Chem* 2003; **278**:24874–24880.
7. Verdelis K, Ling Y, Sreenath T *et al*. DSPP effects on in vivo bone mineralization. *Bone* 2008; **43**:983–990.
8. Xiao S, Yu C, Chou X *et al*. Dentinogenesis imperfecta I with or without progressive hearing loss is associated with distinct mutations in DSPP. *Nat Genet* 2001; **27**:201–204.
9. Zhang X, Zhao J, Li C *et al*. DSPP mutation in dentinogenesis imperfecta Shields type II. *Nat Genet* 2001; **27**:151–152.
10. Qin C, Brunn JC, Cadena E *et al*. The expression of dentin sialophosphoprotein gene in bone. *J Dent Res* 2002; **81**:392–394.
11. Qin C, Brunn JC, Cadena E, Ridall A, Butler WT. Dentin sialoprotein in bone and dentin sialophosphoprotein gene expressed by osteoblasts. *Connect Tissue Res* 2003; **44**(suppl 1):179–183.
12. Baba O, Qin C, Brunn JC *et al*. Detection of dentin sialoprotein in rat periodontium. *Eur J Oral Sci* 2004; **112**:163–170.
13. Alvares K, Kanwar YS, Veis A. Expression and potential role of dentin phosphophoryn (DPP) in mouse embryonic tissues involved in epithelial-mesenchymal interactions and branching morphogenesis. *Dev Dyn* 2006; **235**:2980–2990.
14. Ogbureke KU, Fisher LW. Expression of SIBLINGs and their partner MMPs in salivary glands. *J Dent Res* 2004; **83**:664–670.
15. Ogbureke KU, Fisher LW. Renal expression of SIBLING proteins and their partner matrix metalloproteinases (MMPs). *Kidney Int* 2005; **68**:155–166.
16. Ogbureke KU, Fisher LW. SIBLING expression patterns in duct epithelia reflect the degree of metabolic activity. *J Histochem Cytochem* 2007; **55**:403–409.
17. Prasad M, Zhu Q, Sun Y *et al*. Expression of dentin sialophosphoprotein in non-mineralized tissues. *J Histochem Cytochem* 2011; **59**:1009–1021.
18. Prasad M, Butler WT, Qin C. Dentin sialophosphoprotein in biomineralization. *Connect Tissue Res* 2010; **51**:404–417.
19. Sun Y, Gandhi V, Prasad M *et al*. Distribution of small integrin-binding ligand, N-linked glycoproteins (SIBLING) in the condylar cartilage of rat mandible. *Int J Oral Maxillofac Surg* 2010; **39**:272–281.
20. Page RC, Schroeder HE. Current status of the host response in chronic marginal periodontitis. *J Periodontol* 1981; **52**:477–491.
21. Liang S, Hosur KB, Domon H, Hajishengallis G. Periodontal inflammation and bone loss in aged mice. *J Periodontol Res* 2010; **45**:574–578.
22. Ye L, Zhang S, Ke H, Bonewald LF, Feng JQ. Periodontal breakdown in the Dmp1 null mouse model of hypophosphatemic rickets. *J Dent Res* 2008; **87**:624–629.
23. Feng JQ, Ward LM, Liu S *et al*. Loss of DMP1 causes rickets and osteomalacia and identifies a role for osteocytes in mineral metabolism. *Nat Genet* 2006; **38**:1310–1315.
24. Narayanan K, Ramachandran A, Hao J *et al*. Dual functional roles of dentin matrix protein 1. Implications in biomineralization and gene transcription by activation of intracellular Ca²⁺ store. *J Biol Chem* 2003; **278**:17500–17508.
25. Qin C, D'Souza R, Feng JQ. Dentin matrix protein 1 (DMP1): new and important roles for biomineralization and phosphate homeostasis. *J Dent Res* 2007; **86**:1134–1141.
26. Feng JQ, Huang H, Lu Y *et al*. The Dentin matrix protein 1 (Dmp1) is specifically expressed in mineralized, but not soft, tissues during development. *J Dent Res* 2003; **82**:776–780.
27. Gluhak-Heinrich J, Ye L, Bonewald LF *et al*. Mechanical loading stimulates dentin matrix protein 1 (DMP1) expression in osteocytes in vivo. *J Bone Miner Res* 2003; **18**:807–817.
28. Yang W, Kalajzic I, Lu Y *et al*. In vitro and in vivo study on osteocyte-specific mechanical signaling pathways. *J Musculoskelet Neuronal Interact* 2004; **4**:386–387.
29. Yang W, Lu Y, Kalajzic I *et al*. Dentin matrix protein 1 gene cis-regulation: use in osteocytes to characterize local responses to mechanical loading in vitro and in vivo. *J Biol Chem* 2005; **280**:20680–20690.
30. Jadowiec J, Koch H, Zhang X, Campbell PG, Seyedain M, Sfeir C. Phosphophoryn regulates the gene expression differentiation of NIH3T3 MC3T3-E1 human mesenchymal stem cells via the integrin/MAPK signaling pathway. *J Biol Chem* 2004; **279**:53323–53330.
31. Jadowiec J, Zhang X, Li J, Campbell PG, Sfeir C. Extracellular matrix-mediated signaling by dentin phosphophoryn involves activation of the Smad pathway independent of bone morphogenetic protein. *J Biol Chem* 2006; **281**:5341–5347.

This document is a scanned copy of a printed document. No warranty is given about the accuracy of the copy. Users should refer to the original published version of the material.